Journal of Applied Polymer Science

Fabrication and characterization of hydrophilic poly(ε-caprolactone)/pluronic P123 electrospun fibers

M. M. Mirhosseini, V. Haddadi-Asl, S. Sh. Zargarian
Department of Polymer Engineering and Color Technology, Amirkabir University of Technology, Tehran, Iran
Correspondence to: V. Haddadi-Asl (E-mail: haddadi@aut.ac.ir)

ABSTRACT: Poly(ε-caprolactone) (PCL) has been widely investigated for tissue engineering applications because of its good biocompatibility, biodegradability, and mechanical properties; however hydrophobic nature of PCL has been a colossal obstacle toward achieving scaffolds which offer satisfactory cell attachment and proliferation. To produce highly hydrophilic electrospun fibers, PCL was blended with pluronic P123 (P123) and the resulted electrospun scaffolds physiochemical characteristics such as fiber morphology, thermal behavior, crystalline structure, mechanical properties, and wettability were investigated. Moreover molecular dynamic (MD) simulation was assigned to evaluate the blended and neat PCL/water interactions. Presence of P123 at the surface of electrospun blended fibers was detected using ATR-FTIR analysis. P123 effectiveness in improving the hydrophilicity of the scaffolds was demonstrated by water contact angel which experienced a sharp decrease from 132° corresponding to the neat PCL to almost 0° for all blended samples. Also a steady increase in water uptake ratio was observed for blended fibers as P123 content increased. The 90/10 blend ratio had the maximum tensile strength, elongation at break and crystallinity percentage. Therefore 90/10 blend ratio of PCL/P123 can balance the mechanical properties and bulk hydrophilicity of the resulted electrospun scaffold and would be a promising candidate for tissue engineering application. © 2016 Wiley Periodicals, Inc. J. Appl. Polym. Sci. **2016**, *133*, 43345.

KEYWORDS: elastomers; resins; thermal properties; thermosets; mechanical properties

Received 14 October 2015; accepted 14 December 2015
DOI: 10.1002/app.43345

INTRODUCTION

Electrospinning is an ingenious technique which can produce polymeric fibers with diameters ranging from 5 nanometer (nm) to 1 micrometer (μm) under a high-voltage electrostatic field operating between a metallic capillary syringe and an electrically earthed collector. With high surface to volume ratio and porosity, electrospun scaffolds mimic the natural extracellular matrix and enhance the adhesion, proliferation, and growth of cells.[1,2] A wide range of natural and synthetic polymeric materials have been successfully electrospun into micro and nanofibrous structures and used as scaffolds for tissue engineering, drug carriers, regenerative medicine, and membranes for refinement purposes or fuel cells.[3,4]

PCL, a synthetic and semi-crystalline polymer with repeating $O-(CH_2-)_5-CO-$ units, has been extensively used in tissue engineering because of its good biocompatibility, biodegradability, mechanical properties, and ease of processing and undergoes hydrolysis without producing any toxic byproducts. However, the main barrier for using PCL particularly as scaffolding materials is its hydrophobic character.[5,6]

In the field of tissue engineering, the nature of scaffold surface, such as chemical functionalities, charge, roughness, and wettability has been shown to be critical for cell adhesion and proliferation.[7–9] The hydrophilized scaffolds yield high initial cell seeding density, homogeneous cell distribution, and fast cell growth. These desirable properties are due to the appropriate absorption/diffusion of cell culture medium into the scaffolds and the existence of specific interaction sites for cellular attachment, all of which are essential for the formation of well-integrated tissues. For the aforementioned reason, hydrophilization of scaffolds has been extensively investigated.[10–12]

To improve the hydrophilicity and physiological activities of hydrophobic substrates, various approaches, including prewetting,[13] surface hydrolysis,[14] surface coating,[15] plasma treatment,[16] surface grafting,[17] and bulk blending[18] have been utilized. Among them, blending with hydrophilic polymers and oligomers is an effective method that has been used to fabricate scaffolds with a wide range of physicochemical features including improved hydrophilicity, good mechanical properties, and enhanced cellular interactions.

In recent years, several attempts have been made to blend numerous hydrophilic polymers and oligomers with hydrophobic PCL. For instances, Kim *et al.*[19] have shown that incorporation of lactic acid in PCL fibers by means of simple blending

could easily accelerate the rate of biodegradation of PCL fibers due to the acid-catalyzed hydrolytic degradation of PCL.

Effect of merging gelatin with PCL nanofibrous mat has been studied by Ghasemi-Mobarakeh *et al.*[20] They reported that PCL/gelatin nanofibrous scaffolds enhance the nerve differentiation and proliferation in comparison with pristine PCL nanofibrous scaffold. Kim *et al.*[21] proposed that blending PCL with polyvinyl alcohol (PVA) enhances cell attachment and proliferation due to the wettability of PCL/PVA electrospun scaffold. Zhang *et al.*[22] have shown that PCL/collagen fibrous scaffolds not only provide a suitable environment for the growth and viability of L929 fibroblasts but also increase the ultimate tensile strength of the prepared samples in comparison with the neat PCL fibrous scaffold. A study by Kim *et al.*[23] revealed the efficacy of poly(*N*-vinyl-2-pyrrolidone) blended PCL electrospun fibers for tissue engineering application. Their study demonstrated that changing the mat hydrophobicity alters the rate of degradation.

Pluronic block copolymers are amphiphilic synthetic polymers, consisting of hydrophilic polyethylene oxide (PEO) and hydrophobic polypropylene oxide (PPO) blocks with a PEO–PPO–PEO arrangement. The block copolymers with different numbers of ethylene oxide and propylene oxide units are characterized by different hydrophilic–lipophilic balance (HLB).[24,25] Pluronic has been studied for pharmaceutical applications such as tissue engineering, diagnosis and drug carriers. Also, due to their amphiphilic characteristic these copolymers display surfactant properties including the ability to interact with hydrophobic surfaces and biological membranes.[26,27]

Many of biocompatible hydrophilic polymers can be blended with PCL in order to tune the resulted blend hydrophilicity, however, the scarcity of solvent systems for dissolution of both polymers (common organic solvent for hydrophobic polymers usually do not dissolve hydrophilic polymers), phase separation between hydrophilic and hydrophobic polymers, and hydrophilic polymer leakage from the blend while immersed in aqueous media, are major drawbacks.[10] Instead, pluronic can be an excellent choice to blend with hydrophobic polymers such as PCL. Hydrophobic blocks of pluronic satisfy the physiochemical requirements of blend miscibility while scaffold hydrophilicity is being affected by the copolymer hydrophilic blocks.

Pluronic has been successfully applied to improve the hydrophilic performance of various hydrophobic polymers. For instance Vasita *et al.*[28] have demonstrated that surface hydrophobicity of poly(lactide-*co*-glycolide) (PLGA) fibers can be moderated by electrospinning of PLGA with small amounts of Pluronic F108. Recently, poly(ε-caprolactone-*co*-lactide) (PLCL) was blended with Pluronic F127 by Liu *et al.*[29] Compared with PLCL, improved cell adhesion and proliferation of adipose-derived stem cells was exhibited on all PLCL/Pluronic blended scaffolds. Lately, Kurusu and Demarquette[30] have shown that by blending a triblock copolymer composed of styrene and ethylene-co-butylene blocks (SEBS) with 20 wt % of amphiphilic Pluronic F127, it was possible to obtain superhydrophilic mats and maintain mechanical flexibility.

Therefore, the aim of this work is to investigate the effect of P123 introduction into PCL electrospun fibers on hydrophilicity, thermal behavior, crystallinity and mechanical properties of the resulted scaffolds. These scaffolds fabricated at different ratio by means of electrospinning. The surface morphology and composition of electrospun fibers were studied by SEM imaging and ATR- FTIR analyses. In addition, changes in crystalline structures, thermal behavior and mechanical properties of electrospun PCL and P123 fibers when presented in blend were investigated through XRD patterns, DSC thermograms and stress–strain curves. Surface and bulk hydrophilic properties were studied by contact angle and swelling ratio measurements. Furthermore, to evaluate the influence of surface hydrophilization on the polymer/water interactions at atomic level, molecular dynamic simulations were designed and evaluated.

EXPERIMENTAL

Materials

PCL with $Mw = 80,000$, and P123 with $Mn = 5800$ were purchased from Sigma–Aldrich. Methanol (CH_3OH) and chloroform ($CHCl_3$) used for electrospinning were obtained from Merck. All reagents were of analytical grade and were used as received.

Electrospinning Process

Polymer solutions with fixed concentration of 8.5 wt % were prepared by dissolving the mixture of PCL and P123 in chloroform/methanol at different ratio (100/0, 95/5, 90/10, 85/15, 80/20, and 75/25). A proportion of chloroform and methanol (3:1) was chosen to balance the low and high dielectric constant values of chloroform and methanol, respectively. The solutions were magnetically stirred at room temperature for 24 h to obtain complete dissolution. Scaffolds were produced by electrospinning; set-up consisted of a high voltage supply, a syringe pump and a collector. For scaffold fabrication, each sample of prepared solutions was placed in a syringe (5 mL) topped with a 22 gauge needle and then connected to 14 kV voltage. The mass flow rate was 1.4 mL h^{-1}, and the distance between the tip and the collector was 14 cm. Electrospinning was carried out at room temperature (23°C ± 2°C). All electrospun fibers were deposited on a collector consisting of aluminum foil to form a thin fibrous membrane. The fibrous membranes were placed in vacuum drying at room temperature to completely remove any solvent residue.

Characterization of Electrospun Scaffolds

The morphology of electrospun structures was determined by scanning electron microscopy (SEM) (SERON AIS-2100, South Korea) using 15 kV accelerating voltage. The samples were coated with gold using a sputter coater before SEM imaging. The average fiber diameter and corresponding size distribution were analyzed by measuring ~200 fibers presented in SEM micrographs using an image analyzer (Image J, developed by the National Institute of Health, USA).

Surface chemical analysis of P123 pristine and PCL/P123 fibrous scaffolds were performed using ATR-FTIR spectroscopy with 45 degree ZnSe crystal (Nexus 670 spectrometer, Thermo Nicolet, USA) in a range of 4000–600 cm^{-1}.

Differential scanning calorimetry (DSC) experiments were conducted with a Flash DSC 1 of Mettler-Toledo, in order to evaluate

the thermal properties of the PCL and PCL/P123 blended fibers. The experiments were conducted at a constant heating rate of 10°C min^{-1} on samples (15–20 mg) packed in aluminum pans under nitrogen flow. The samples were heated in two stages. First, the samples were heated to 120°C and kept at that temperature for 5 min to erase the thermal history. Afterward they were cooled to −60°C and then reheated again to 120°C. The melting temperature (T_m) and the melting enthalpy (ΔH) of PCL and PCL/P123 blended fibers were determined from the heating scans. The crystallinity percentage ($\%X_c$) can be calculated by applying the equation:

$$\% X_c = \left(\frac{\Delta H}{\Delta H_u^{\circ} w}\right) \times 100 \quad (1)$$

where ΔH_u° is the melting enthalpy of 100% crystalline PCL (139 J g^{-1})[31] and w is the weight fraction of PCL in the blend.

X-ray diffraction (XRD) spectra were prepared on an X-ray diffraction instrument (Siemens D5000) with a Cu target ($\lambda = 0.1540$ nm) at room temperature. The samples were scanned from 2 to 85° at the step scan mode by a scanning rate of 0.2° per minute. The system consists of a rotating anode generator, and operated at 35 kV and a current of 20 mA.

Mechanical properties of different scaffolds were performed using an electromechanical tensile tester (Instron 5566, Elancourt, France). Rectangular specimens with a length of 20 mm and a width of 5 mm were manually cut from electrospun samples with a thickness ranging from 100 to 150 μm. All samples were mounted between two holders at a distance of 2 cm. The stress strain curves of these materials were the plotted from the load-deformation curves recorded at a stretching speed of 5 mm min^{-1}.

To determine the influence of P123 on the hydrophilicity of PCL, water contact angle test was carried out using a commercial drop shape analysis system (Data Physics OCA-15 plus, equipped with CCD camera and imaging software). The 2 × 2 cm^2 freshly prepared electrospun mesh was kept under vacuum for 24 h to avoid surface impurity. The mesh was then attached to a glass slide for contact angle measurements. In each measurement, a droplet of deionized water (4 μL) was pipetted onto the membrane surface. Images of the water droplet were taken using a high speed digital camera and the values of contact angle were calculated from the images.

The water uptake and swelling properties of the PCL and PCL/P123 blended fibrous mats were analyzed with swelling ratio test. Samples were cut into small quadrangular pieces at ~2 × 2 cm^2 which were accurately weighed (W_o) and immersed in distilled water. The samples were then pulled out at specific time intervals and excess water was removed from the samples before obtaining the wet weight (W_s). The percentage swelling ratio was calculated using the equation:

$$Swelling\ ratio\,(\%) = \left[\frac{W_s - W_o}{W_o}\right] \times 100 \quad (2)$$

Results were expressed by the means of the measurements ($n = 3$) with the error bars representing the standard deviation.

Simulation Details

MD simulations were adjusted with the commercial molecular modeling software package Materials Studio 4.3 from Accelrys Software Inc. (San Diego, CA). For computing interatomic interactions the COMPASS (condensed-phase optimized molecular potentials for atomistic simulation studies) force field was selected. The COMPASS force field has the ability to minimize and calculate the structural and conformational properties of polymeric systems. The functional form of COMPASS force field terms are given in reference.[32] It should be noted that, the COMPASS force field has been already applied to a wide range of polymeric materials such as PCL and pluronic.[33–35] Firstly, PCL and P123 chains were built from their repeat units by Build module, and then cubic simulation boxes were constructed using Amorphous cell module. The PCL and PCL/P123 systems are in a relatively high-energy state, hence minimizations should be performed to remove unwanted interactions and to attain the lowest energy state. For this purpose, polymer chains were optimized by the steepest descent and conjugate gradient method. During the procedure of structure optimization, the maximum number for the minimization was 10,000. MD simulations were conducted for 1000 picosecond (ps) at NPT (constant pressure P and constant temperature T) condition until the box size became constant and then using NVT (constant volume V and constant temperature T) condition for 1000 ps equilibrium was reached. To determine the effect of P123 on the hydrophilicity of PCL, the water/PCL and water/PCL/P123 systems were created. For these systems, the minimized molecular structure of the polymer chains was used to build a bottom layer. On top of this layer, a water layer was added. To omit the undesirable contacts including overlapping and close contact, a 20,000 step energy minimization was adopted using the steepest descent and conjugate gradient method. To calculate interaction of the water layer with the polymer chains, MD simulation was performed using an NPT ensemble for 2000 ps, where the pressure and temperature were controlled by the Anderson thermostat (298°K) and Berendsen barostat (0.0001 GPa), respectively. Discover module was used for minimization and dynamic parts. The integration of the equations of motion has been performed by means of the Verlet velocity time integration method with a time step of 1 femtosecond (fs). The initial velocities of the atoms were assigned using a Maxwell–Boltzmann distribution at the desired temperature and pressure. A cutoff radius of 1.25 nm was used for Lennard–Jones interactions and Ewald summation to compute long-range electrostatic interactions.

RESULTS AND DISCUSSION

Fiber Morphology

Figure 1 illustrates SEM images of PCL and PCL/P123 electrospun mats, average fiber and bead diameter and number of counted beads. Existence of P123 in the electrospinning solution did not affect morphology of fibers, e.g. fiber smoothness and mat integrity. However average fiber diameter experienced a surge from 410 to 560 nm and then a reduction to 310 nm when P123 content increased in the blend. The non uniformity of fiber diameter is an inherent characteristic of electrospun PCL scaffolds probably resulted from electrospinning solution

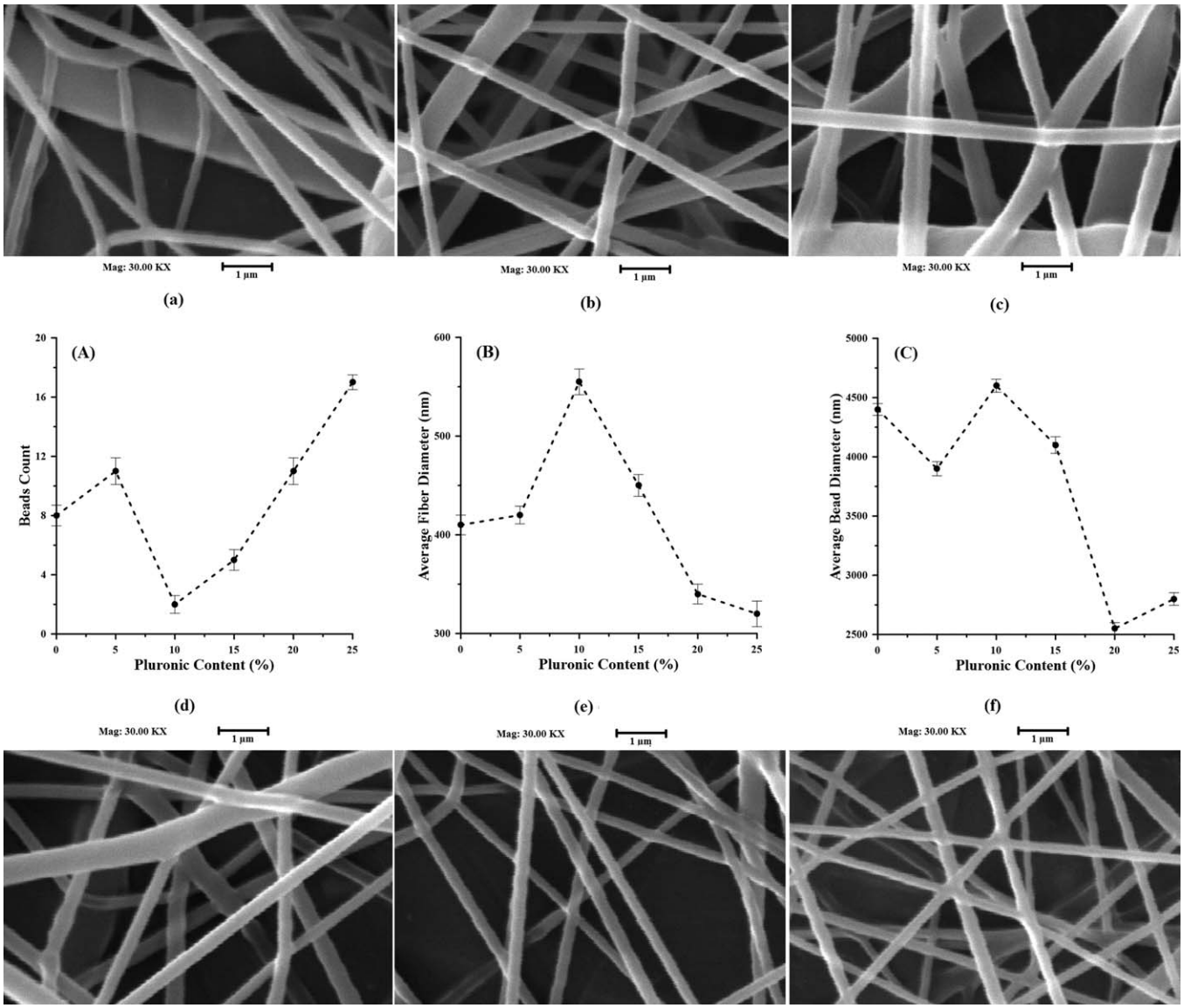

Figure 1. SEM images of PCL/P123 fibers with different blend ratio (a) 100/0, (b) 95/5, (c) 90/10 (d) 85/15, (e) 80/20, and (d) 75/25. (A) Number of counted beads, (B) Average fiber and (C) Bead diameter.

conductivity.[36,37] However, the bimodal characteristic of electrospun PCL fibers changed to unimodal distribution when blended with P123. This observation may be caused by different factors which control fiber diameter for blended polymers. Surface tension is a dominant factor in fiber diameter determination. Adding a polymer with much lower molecular weight to a proposed blend has a drastic effect on the viscoelastic forces which diminishes them and as a result surface tension would play a strong role on the morphology of the resulting fibers.[38,39] Miscibility of two polymeric materials also has a strong effect on the average fiber diameter. At lower concentrations of P123, achieving a miscible blend is more feasible, therefore fiber characteristics is more close to the pristine PCL fibrous mat. Beaded fiber appeared more frequently in the electrospun mat once PCL content decreased; with one exception for 90/10 blend which possessed the lowest amount of beads on fiber (two beads observed in the related SEM photo containing ~150 fibers). However, average bead diameter decreased dramatically from 90/10 blend ratio forward (from 4600 nm to almost 2500 nm). Fibers produced from polymer solutions of lower concentration or viscosity often possess low mechanical properties which may have arisen from low chain entanglement.[40–42] PCL chain length is roughly 20 times bigger than that of a P123 when fully stretched. As a result, in blends with low PCL concentration, chain entanglement and total viscosity decrease drastically (data not shown). Consequently, during electrospinning process, tangential and polarization stress exerted on the charged jet may yield fibers with low elasticity and therefore smaller beads.

ATR–FTIR Analysis

In systems containing two or more types of materials, the ATR–FTIR is an effective method to analyze surface elements. The presence of P123 blended with PCL on the surface of the fibers can be detected. The ATR-FTIR spectra of P123 and PCL/P123

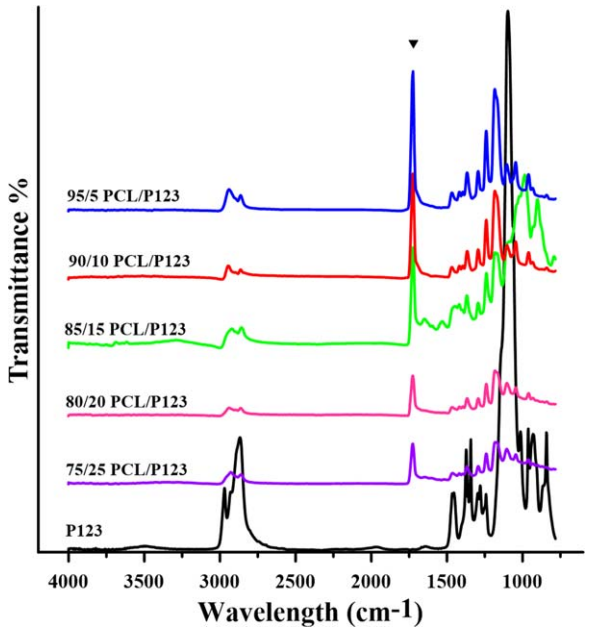

Figure 2. ATR-FTIR spectra of P123 and PCL/P123 electrospun scaffolds with different blend ratio. [Color figure can be viewed in the online issue, which is available at wileyonlinelibrary.com.]

blended fibers are shown in Figure 2. The PCL-related stretching modes are represented by the peaks at 2943 cm^{-1} (asymmetric CH_2 stretching), 2866 cm^{-1} (symmetric CH_2 stretching), 1721 cm^{-1} (C═O stretching), 1294 cm^{-1} (C—O and C—C stretching), 1170 cm^{-1} (symmetric C—O—C stretching) and 1240 cm^{-1} (asymmetric C—O—C stretching).[43] The characteristic peaks of P123 in blend fibers are totally overlapped by PCL peaks. Indeed, ATR-FTIR spectra of the PCL and PCL/P123 blends display similar patterns, indicating that no significant change in the molecular structure toke place upon blending. However, it is noted that the distinctive band attributed to the carbonyl groups of PCL (at 1721 cm^{-1}) decreases in quantity with the increase in P123 content in blends. This quantity, however, remains constant at 80/20 and 75/25 blend ratio indicating a saturation percentage of P123 on the fiber surface.

Thermal Behavior

The relationship between thermal behavior and physicochemical properties of the electrospun fibers such as crystallinity percentage and polymeric chains interaction has been well recognized. The relevant thermograms of the PCL/P123 fibers with different blend ratio during first and second heat scans are shown in Figure 3. Pristine PCL electrospun fibers show an endothermic peak related to the melting of the crystalline phase in a temperature range between 30–70°C, with a maximum at 59°C. When P123 is present in the fiber composition another endothermic peak appears around 31–32°C. From 85/15 blend ratio forward, another melting peak takes form in a temperature range between 42 and 43°C. This peak becomes more pronounced when P123 content in blend increases.

In semicrystalline block copolymers, the appearance of more than one melting transition can be related to chain folding. That is, crystals with different numbers of folds have different melting transition. Extended or once-folded chains are the least folded crystals and have a higher melting transition in comparison to that of crystals containing more highly folded chains.[44,45] During electrospinning process, it is evident that solvent evaporates much faster from the surface of stretching jet and polymer chains in its core have more time to fold and form crystals. Moreover, chains which are closer to the jet surface experience more tangential and polarization stress hence stress induced crystallization occurs more favorably in the jet surface.[46,47] Consistent with these arguments, for P123 thermal properties, it can be concluded that the endothermic peak which happens at lower temperature can be associated to the crystals with highly folded chains whereas the peak which occurs at higher temperature belongs to the least folded crystals. As mentioned before, the latter endothermic peak becomes more recognizable as P123 content in the blend increases. This observation may be due to the accumulation of P123 at the fiber surface which yields stress induced crystals of once-folded chains with higher melting transition. Another interesting observation can be made from DSC thermograms when the history of electrospinning process omitted from the solidified PCL/P123 blend. This time only one melting transition peak can be detected for the P123 crystals. Also the mentioned peak shifts towards lower temperatures which correlate to the crystals with highly folded chains. It can be concluded that extended crystals of P123 resulted from the electrospinning process. The area under the DSC thermogram curves for PCL melting transition has been calculated. The difference between the mentioned area during first and second heat scans was obtained by following equation and results were plotted versus different blend ratio and presented in Figure 4. Moreover stated quantities, crystalline percentages and melting temperatures were tabulated in Table I:

$$\delta = \Delta H' - \Delta H' \tag{3}$$

$\Delta H'$ and $\Delta H''$ refer to the area under the endothermic peaks of PCL in blend with and without electrospinning process history, respectively. When plotted against different weight percentages of PCL in blend, both $\Delta H'$ and $\Delta H''$ follow a same declining trend with an exception at 90/10 blend ratio. It is obvious that the area under the PCL melting peak in blend thermograms should decrease at higher P123 ratio in blends. The mentioned exception may be caused by synergistic interactions between PCL and P123 chains at 90/10 blend ratio which resulted in higher amounts of crystalline percentage.

Surprisingly δ trails a different path from $\Delta H'$ and $\Delta H''$. It decreases noticeably as P123 content in blend increases and then remains constant from 80/20 blend ratio forward. The optimum observed at 90/10 blend ratio in $\Delta H'$ and $\Delta H''$ diagrams fades in δ trend. The difference between the PCL melting enthalpy of first and second heat scans plummeted to almost zero at 80/20 blend ratio stating the omission of electrospinning process effect from thermograms of the PCL/P123 fibers.

As it was mentioned before, solvent evaporates much fast from the exposed surface of a stretching jet and therefore polymer chains in its core have more time to fold and form crystals. The difference between $\Delta H'$ and $\Delta H''$ lays solely on the electrospinning process effect. In other words, if the history of electrospinning erased from

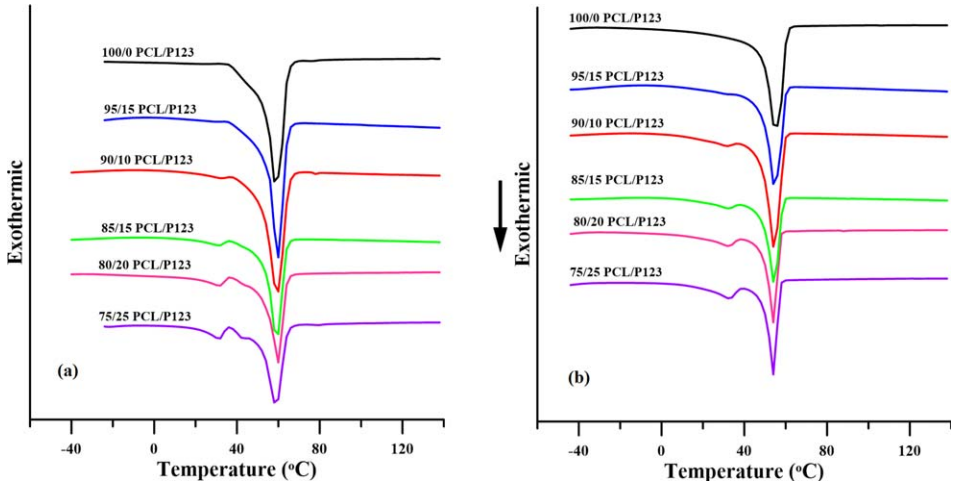

Figure 3. DSC thermograms of the PCL/P123 scaffolds with different blend ratio during (a) first and (b) second heat scans. [Color figure can be viewed in the online issue, which is available at wileyonlinelibrary.com.]

the PCL/P123 blend; the quantities of $\Delta H'$ and $\Delta H''$ would be equal. Vasita *et al.*[28] reported a surface enrichment value for PF108 on electrospun nanofibers when blended with different amounts of PLGA. They proposed that by increasing the weight percentage of PF108 in PLGA/PF108 polymeric blend, the excess amount of the triblock would be most likely resides within the bulk of the electrospun nanofibers. This means after a certain ratio of PF108 in blend, excess number of PF108 chains would not experience the fast solvent evaporation and forced crystallization; they form crystals with no electrospinning process history. In this study the surface enrichment value for P123 can be deduced from δ diagram. Low quantities of variable δ from 80/20 blend ratio forward, points to the surface enrichment of P123 in the electrospun PCL/P123 fibers. Considering that PCL and P123 is less miscible at higher ratio of blending; at 80/20 blend ratio, excess amount of P123 triblock solidifies in the fibers core, therefore PCL ratio at surface remains constant. This is in line with ATR-FTIR data of the PCL carbonyl groups peak intensity. There, mentioned quantity remained constant at 80/20 and 75/25 blend ratio; pointing to the proposed saturation percentage of P123 on the fiber surface.

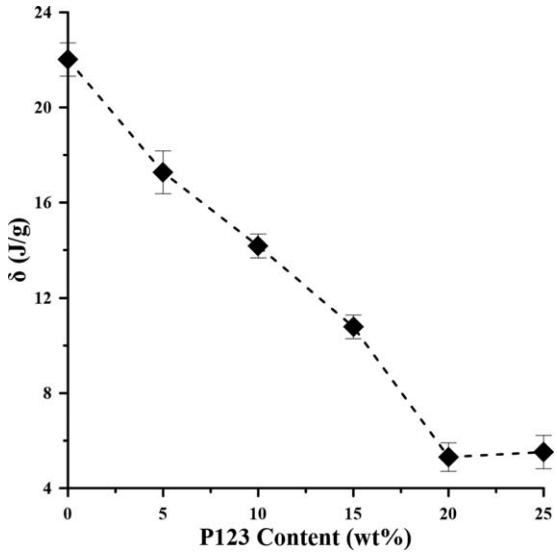

Figure 4. δ versus P123 content in blend with PCL.

XRD

To study the crystalline structures of PCL and PCL/P123 blend, XRD patterns of prepared scaffolds are presented in Figure 5. As seen, the two diffraction peaks located at 21.4° and 23.6° correspond to the (110) and (200) crystallographic planes of the PCL.[48] The absence of a distinguishable diffraction peak in the XRD pattern of P123 indicates that this polymer is amorphous. At 95/5 blend ratio, a new peak appears around 21° which suggests possible crystalline domains of P123 PPO segments and PCL chains; pointing to good polymer miscibility at this ratio. As the P123 content increases, the crystalline characteristics of the constitutive components of PCL remain, as evidenced from the presence of their respective typical crystalline peaks. Albeit, the intensity of peak at 2θ 21.4° and 23.6° gradually decreases, suggesting that the crystallinity of PCL reduces with the addition of P123. In comparison with the pristine PCL fibers, the two characteristic peaks at 21.4° and 23.6° shift slightly to higher angles for 95/5 and 90/10 blend ratio, indicating a possible decrease in the length of PCL crystal stacks. This may be due to the restraining effects of P123 triblock when blended with hydrophobic PCL chains which prevents the formation of large crystal domains of the latter. This postulation is in line

Table I. Thermal Properties of PCL Pristine and in Blend with P123

	First heat scan			Second heat scan		
PCL/P123 blend ratio	$\Delta H'$ (J g^{-1})	$\%X_c$	T_m (°C)	$\Delta H''$ (J g^{-1})	$\%X_c$	T_m (°C)
100/0	75	54	58.4	53	38	55.2
95/5	66	49	59.96	49	37	54.4
90/10	67	53	60.13	52	41	54.03
85/15	46	39	59.96	34	28	54.03
80/20	37	32	60.03	32	28	53.86
75/25	36	33	58.53	31	29	53.96

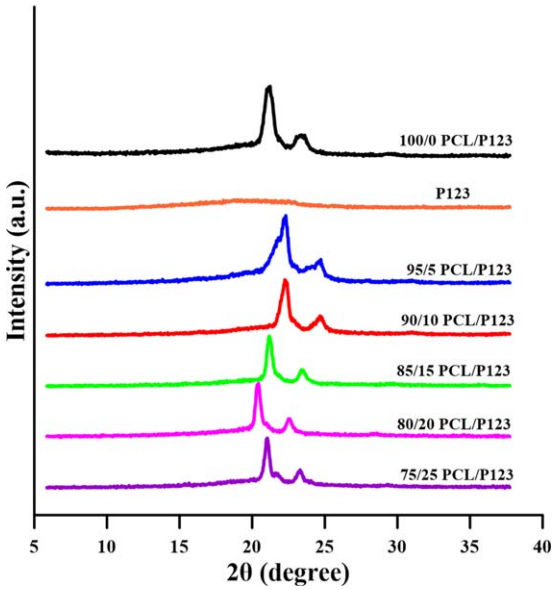

Figure 5. XRD patterns of P123 and PCL/P123 scaffolds with different blend ratio. [Color figure can be viewed in the online issue, which is available at wileyonlinelibrary.com.]

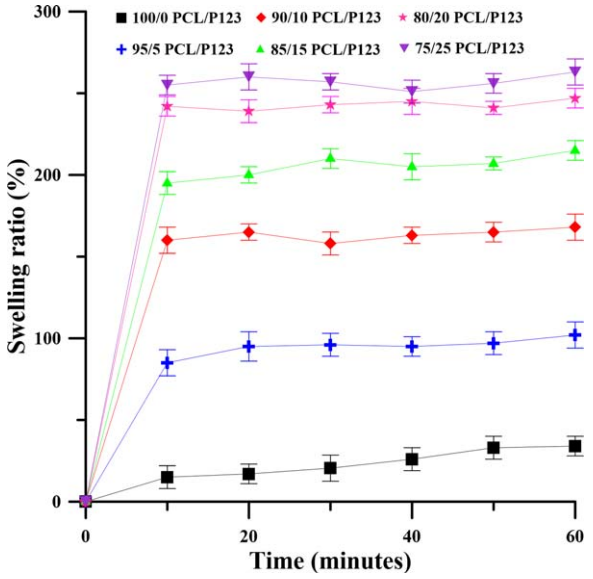

Figure 7. The swelling ratio of electrospun PCL/P123 scaffolds with different blend ratio. [Color figure can be viewed in the online issue, which is available at wileyonlinelibrary.com.]

with our previous observation of PCL/P123 fibers thermograms. There, an exception at 90/10 blend ratio in $\Delta H'$ and $\Delta H''$ trend was considered as a synergistic interaction between PCL and P123 chains which can increase the crystallinity percentage. Combining these two assumptions, it can be concluded that blends of P123 and PCL have an optimum where smaller but more frequent PCL crystalline regions form.

Water Contact Angle Analysis

To investigate the surface hydrophilicity or hydrophobicity of PCL and PCL/P123 scaffolds water contact angle measurement was performed. It has been well established that the water contact angle depends on the topographic patterns and chemical composition of the sample and reveals its wettability. In the case of the electrospun scaffolds, the influence of bead shape and fiber diameter on scaffold wettability has been fully demonstrated.[49,50] These characteristics become important when dealing with protein absorption and cell attachment of the sample. In general, a contact angle between 0° and 30° defines a hydrophilic surface whereas less hydrophilic surfaces show a contact angle up to 90°. Hydrophobic materials possess a contact angle more than 90°.[51] As shown in Figure 6 PCL fibrous mat has a contact angel of 132° indicating that pristine PCL possesses hydrophobic characteristic. The presence of CH_2 groups in the backbone of PCL chains is the main reason of its hydrophobic property. The water contact angle dramatically decreases to 0° after introducing 5 wt % P123. Moreover, all of PCL/P123 scaffold with compositions of 90/10, 85/15, 80/20, and 75/25 exhibit a contact angle of 0°, which indicates their good hydrophilicity. The incorporation of P123 significantly increases the hydrophilicity of the scaffolds and diminishes the influence of the other factors such as fiber morphology on the scaffold wettability. The methyl groups of P123 and ethyl groups of PCL can form possible hydrophobic interactions. These interchain interactions inhibit the incorporation of PEO blocks of P123 into the PCL chains thus forcing them toward the surface. In other words, P123 triblock can be anchored to the hydrophobic surface of PCL by PPO blocks and PEO blocks assemble into a brushlike formation in contact with water.[28,30] Cell attachment and proliferation can be affected to a great extent by the improved hydrophilicity of blended PCL with P123.

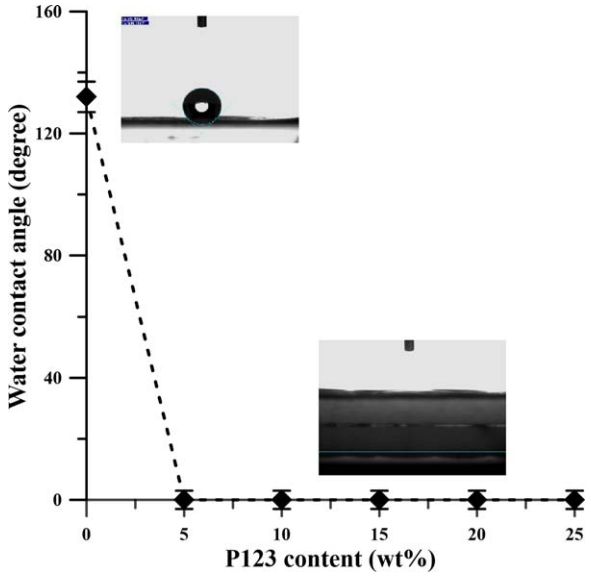

Figure 6. Water contact angle of electrospun PCL/P123 scaffolds with different blend ratio (Inset: camera photos of water droplet on related scaffolds). [Color figure can be viewed in the online issue, which is available at wileyonlinelibrary.com.]

Swelling Test

To expand the study of P123 hydrophilic effect, the water uptake of the electrospun PCL and PCL/P123 blended fibrous scaffolds was measured and presented in Figure 7. As seen, PCL

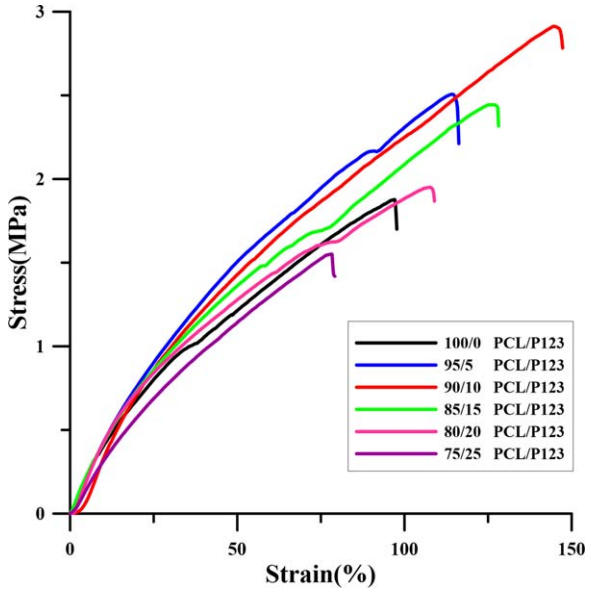

Figure 8. Stress–strain curves of electrospun PCL/P123 scaffolds with different blend ratio. [Color figure can be viewed in the online issue, which is available at wileyonlinelibrary.com.]

fibrous scaffold has the lowest ratio of the water uptake because of its hydrophobic nature in comparison with the blended samples. However water absorption rate of the PCL fibrous scaffold is equal to other blended samples. Swelling ratio experiences a drastic surge from 20% to almost 100% after introducing only 5 wt % P123 to the PCL solution. Water uptake percentage increases linearly with further addition of P123 to the blend with a maximum at 260% swelling ratio for 75/25 blend ratio. Because of the electrospun scaffolds fibrous nature, prepared samples demonstrated rapid swelling characteristic and within 10 min, maximum water adsorption capacity reached. It is noteworthy that difference between 75/25 and 80/20 blend ratio water uptake is considerably lesser than other consecutive blend pairs suggesting an upcoming equivalency in water uptake capacity. This may be due to the dissolution of the excess P123 at higher blending ratio from fibrous structure in water; causing water uptake to remain constant.

Mechanical Properties Evaluation

The influence of P123 addition to the polymeric blend of PCL/P123 on the mechanical properties of fibrous mats was investigated by tensile testing. It is noteworthy that the mechanical properties of the fibrous mats play an important rule on its successful application in tissue engineering. The typical tensile stress–strain curves of PCL and PCL blended with P123 fibrous mats are shown in Figure 8. An overall survey on the stress-strain curves reveals that the presence of P123 in the polymeric blend improves both elongation at break and tensile strength of the resulted electrospun fibers, however 75/25 blend ratio is an exempt. Again 90/10 blend ratio provides an excellent characteristic in comparison to the other prepared samples and points to an optimum in the mechanical properties of the blended fibers. Lim *et al.*[41] stated in their study that higher degree of molecular orientation and crystallinity of the electrospun fibers yields fibrous mats with superior stiffness and strength. From thermograms of the PCL/P123 fibers it was established that the maximum crystallinity percentage belongs to 90/10 blend ratio. Moreover SEM images of the blended fibers revealed a less beaded morphology for the mentioned membrane. Parallel to these observations, 75/25 blend ratio has low crystallinity and numerous beaded fibers among other blends thus lowest tensile strength and elongation at break belongs to this sample. Perhaps the argument provided by Zhang *et al.*[22] is applicable to these findings. They speculated in their study that collagen is responsible for the effectiveness of the scaffolds in absorbing the energy against an applied load through the higher degree of elongation. Collagen is an amorphous polymer with crystalline similarities to P123. As a matter of fact both P123 and collagen represent broad diffraction peak around 2θ 20°. Thus amorphous structure of P123 can be held responsible for energy absorption against an applied load and a balance exist between

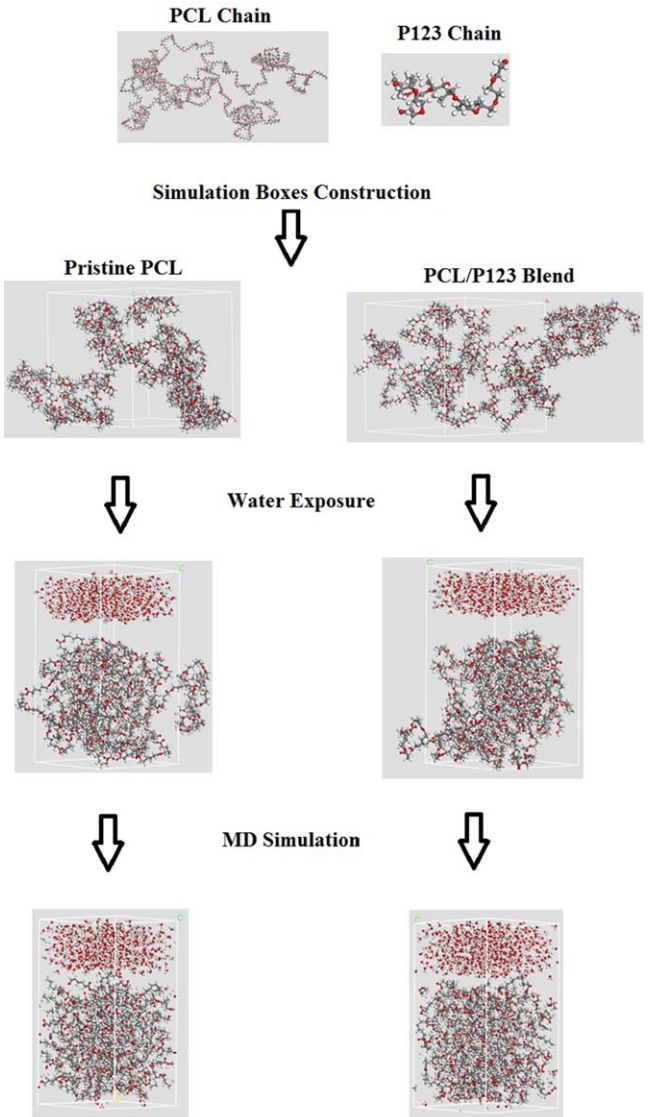

Figure 9. Models for MD simulation of water/PCL and water/PCL/P123 systems. Carbon: gray; hydrogen: white; oxygen: red. [Color figure can be viewed in the online issue, which is available at wileyonlinelibrary.com.]

Table II. The Interaction Energies (kcal mol^{-1}) Between Water and Different Polymer Systems

System	PCL/P123 blend ratio	Number of water molecules	E_{total}	$E_{polymer}$	E_{water}	$E_{interaction}$
PCL/water	100/0	555	−18558.66	−1678.19	−16017.51	−862.95
PCL/P123/water	75/25	555	−18588.28	−1855.22	−15454.43	−1278.61

the improved elongation at break and jeopardized fiber morphology while p123 content in blend increases. Hence, the correlation between the P123 addition to the polymeric blend of PCL/P123 and the altered mechanical properties of the resulted fibrous mats was established.

MD Simulation

In this study the constrained MD was employed to construct the polymer models and to simulate their interactions with water (Figure 9). One of the key steps in the MD simulation is to achieve a fully equilibrated simulated system. It is noteworthy that one of the equilibration conditions for the simulated systems is the study of potential energy and temperature time dependency. In this study and in order to reach equilibrium, both parameters potential energy and temperature were monitored during the MD simulations. Total potential energy and temperature were relatively constant for water/PCL and water/PCL/P123 systems as the time passes. Moreover, the fluctuation in both total potential energy and temperature of the two systems under study was negligible. According to the results, it can be concluded that all simulated systems reached the thermodynamic equilibrium state and the calculated properties were reliable (data not shown). The interaction energy between the model polymers and water molecules were calculated by the summation of all the interaction potentials of the related atoms in polymer chains and water molecules. The interaction energy represents the amount of energy necessary to separate polymer chains from the water surface. In other words, interaction energy symbolizes the attraction or repulsion of polymeric chains toward water molecules. The interaction energy is hence proportional to the difference between the total energy of the system, E_{total}, and the energy of the individual layers, E_{water} and $E_{polymer}$.

$$E_{\text{interaction}} = E_{\text{total}} - \left(E_{\text{polymer}} + E_{\text{water}}\right) \quad (4)$$

The interaction energy of the polymer models with the water molecules in each system was calculated, and results were displayed in Table II. Interactions of water molecules with PCL/P123 chains are about 1.5 times larger than that of the pure PCL (absolute value). By comparing these values and since more negative interaction energy indicates larger attraction, it can be concluded that the interactions between water and PCL/P123 are stronger than those of between water and PCL. These observations are in line with the hydrophilic and hydrophobic characters of PCL/P123 and PCL, respectively.

The Einstein relationship is widely used for obtaining diffusion coefficient from molecular dynamics simulation. When any atom undertakes random Brownian motion in a three dimensional space, its self-diffusion coefficient can be calculated by limiting slope of means square displacement (MSD) as a function of time.

$$MSD = \langle |r(t) - r(0)|^2 \rangle \quad (5)$$

and

$$D = \frac{1}{6N} \lim_{t\to\infty} \frac{d}{dt} \sum_{i=1}^{N} \langle |r_i(t) - r_i(0)|^2 \rangle \quad (5)$$

where $r(t)$ and $r(0)$ denotes the position vector of the atom at time t and $t=0$, respectively. The angular brackets denote averaging of all choices of time origin within a dynamics trajectory.[52] From MSD vs time curve it can be speculated that the diffusion of water molecules is also greatly influenced by the surface hydrophilization (Figure 10). The hydrophobic PCL has a weak influence on the mobility of water molecules. The mobility of water molecules increases with an increase in surface hydrophilicity originated from the formation of new interactions between P123 PEO segments and water molecules. Moreover self-diffusion coefficient of water layer increases almost two-fold after blending P123 with PCL.

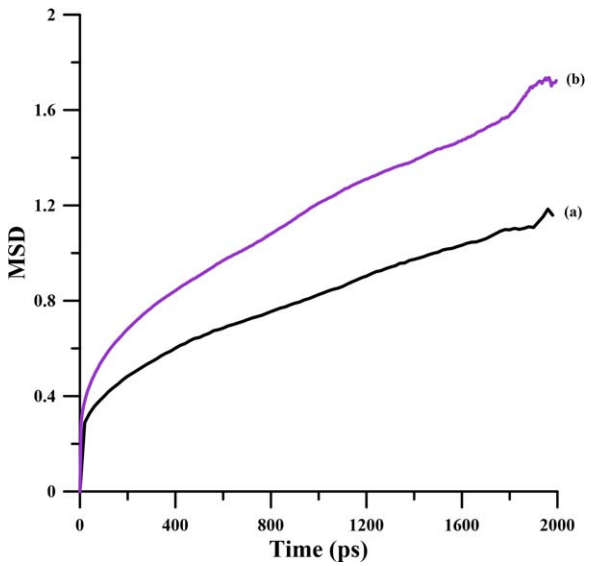

Figure 10. MSD of water layer on different polymer systems: (a) PCL, (b) PCL/P123. [Color figure can be viewed in the online issue, which is available at wileyonlinelibrary.com.]

CONCLUSIONS

Different ratio of P123 was added to the PCL solution and the resulted electrospun fibrous scaffolds were tested in a bid to determine the optimum ratio which holds acceptable mechanical properties and hydrophilicity. Fiber smoothness and mat integrity did not affected by varying the ratio of P123 in the blended solutions however beads on fiber increased as the PCL

content in the electrospinning solutions decreased with an exception for 90/10 blend ratio. ATR–FTIR analysis detected the presence of P123 at the surface of electrospun blended fibers. The stepwise reduction of the peak located at 1721 cm^{-1} affiliated to the carbonyl groups of PCL with increasing P123 quantities in the blended samples proved the presence of P123 at the fiber surface. This reduction plateaued for 80/20 blend ratio forward. Water contact angle reduced drastically and became zero with the incorporation of P123 to PCL fibers even at the lowest blend ratio. Swelling ratio increases stepwise with P123 increment in the blended solutions. A saturation concentration related to the P123 presence on the surface of electrospun fibers was calculated from the DCS thermograms by subtracting the PCL melting enthalpy of the first and second heat scans. It appears that the excess amounts of P123 would reside within the bulk of the electrospun fibers rather than its surface from 80/20 blend ratio forward. Incorporation of P123 into the polymeric solutions improves both elongation at break and tensile strength of the resulted electrospun fibers. The 90/10 blend ratio has the highest mechanical properties which may stem from the optimum synergistic interactions between PCL and P123 polymeric chains at this ratio. MD simulation was successfully predicted the hydrophilicity of the P123/PCL blend. In conclusion, these findings indicate that 90/10 blend ratio of PCL/P123 creates an acceptable balance between mechanical properties and hydrophilicity and potentially reserve a promising place in tissue engineering applications.

REFERENCES

1. Aoki, H.; Miyoshi, H.; Yamagata, Y. *Polym. J.* **2015**, *47*, 267.
2. Zargarian, S. S.; Haddadi-Asl, V. *Iran. Polym. J.* **2010**, *19*, 457.
3. Baiguera, S.; Del Gaudio, C.; Lucatelli, E.; Kuevda, E.; Boieri, M.; Mazzanti, B.; Bianco, A.; Macchiarini, P. *Biomaterials* **2014**, *35*, 1205.
4. Martina, M.; Hutmacher, D. W. *Polym. Int.* **2007**, *56*, 145.
5. Dash, T. K.; Konkimalla, V. B. *J. Controlled Release* **2012**, *158*, 15.
6. Arcana, I. M.; Bundjali, B.; Yudistira, I.; Jariah, B.; Sukria, L. *Polym. J.* **2007**, *39*, 1337.
7. Chang, H. Y.; Huang, C. C.; Lin, K. Y.; Kao, W. L.; Liao, H. Y.; You, Y. W.; Lin, J. H.; Kuo, Y. T.; Kuo, D. Y.; Shyue, J. J. *J. Phys. Chem. C* **2014**, *118*, 14464.
8. Arima, Y.; Iwata, H. *Biomaterials* **2007**, *28*, 3074.
9. Akkas, T.; Citak, C.; Sirkecioglu, A.; Güner, F. S. *Polym. Int.* **2013**, *62*, 1202.
10. Oh, S. H.; Lee, J. H. *Biomed. Mater.* **2013**, *8*, 014101.
11. Lee, J. H.; Khang, G.; Lee, J. W.; Lee, H. B. *J. Colloid Interface Sci.* **1998**, *205*, 323.
12. Song, W.; Mano, J. F. *Soft Matter* **2013**, *19*, 2985 CrossRef][10.1039/c3sm27739a]
13. Mikos, A. G.; Lyman, M. D.; Freed, L. E.; Langer, R. *Biomaterials* **1994**, *15*, 55.
14. Luca, A. C.; Terenghi, G.; Downes, S. *J. Tissue Eng. Regen. Med.* **2014**, *8*, 153.
15. Zhang, L. F.; Sun, R.; Xu, L.; Du, J.; Xiong, Z. C.; Chen, H. C.; Xiong, C. D. *Mater. Sci. Eng. C* **2008**, *28*, 141.
16. de Valence, S.; Tille, J. C.; Chaabane, C.; Gurny, R.; Bochaton-Piallat, M. L.; Walpoth, B. H.; Möller, M. *Eur. J. Pharma. Biopharma.* **2013**, *85*, 78.
17. Sun, H.; Wirsén, A.; Albertsson, A. C. *Biomacromolecules* **2004**, *5*, 2275.
18. Kim, Y. E.; Kim, Y. J. *Polym. J.* **2013**, *45*, 845.
19. Kim, E. K.; Pant, H. R.; Hwang, B. S.; Kim, Y. K.; Kim, H. Y.; Lee, K. M.; Park, C. H.; Kim, C. S. *Polym. Int.* **2014**, *63*, 1212.
20. Ghasemi-Mobarakeh, L.; Prabhakaran, M. P.; Morshed, M.; Nasr-Esfahani, M. H.; Ramakrishna, S. *Biomaterials* **2008**, *29*, 4532.
21. Kim, C. H.; Khil, M. S.; Kim, H. Y.; Lee, H. U.; Jahng, K. Y. *J. Biomed. Mater. Res. B: Appl. Biomater.* **2006**, *78*, 283.
22. Zhang, Q.; Lv, S.; Lu, J.; Jiang, S.; Lin, L. *Int. J. Biol. Macromol.* **2015**, *76*, 94.
23. Kim, G. M.; Le, K. H. T.; Giannitelli, S. M.; Lee, Y. J.; Rainer, A.; Trombetta, M. *J. Mater. Sci. Mater. Med.* **2013**, *24*, 1425.
24. Pitto-Barry, A.; Barry, N. P. *Polym. Chem.* **2014**, *5*, 3291.
25. Kwon, K. W.; Park, M. J.; Hwang, J.; Char, K. *Polym. J.* **2001**, *33*, 404.
26. Hunt, J. A.; Chen, R.; van Veen, T.; Bryan, N. *J. Mater. Chem. B* **2014**, *2*, 5319.
27. Wang, J. Y.; Marks, J.; Lee, K. Y. C. *Biomacromolecules* **2012**, *13*, 2616.
28. Vasita, R.; Mani, G.; Agrawal, C. M.; Katti, D. S. *Polymer* **2010**, *51*, 3706.
29. Liu, N.; Pan, J.; Miao, Y. E.; Liu, T.; Xu, F.; Sun, H. *J. Mater. Sci.* **2014**, *49*, 7253.
30. Kurusu, R. S.; Demarquette, N. R. *Langmuir* **2015**.
31. Wang, X.; Zhao, H.; Turng, L. S.; Li, Q. *Ind. Eng. Chem. Res.* **2013**, *52*, 4939.
32. Jawalkar, S. S.; Aminabhavi, T. M. *Polym. Int.* **2007**, *56*, 928.
33. Li, Y.; Liu, H.; Song, J.; Rojas, O. J.; Hinestroza, J. P. *ACS Appl. Mater. Interfaces* **2011**, *3*, 2349.
34. Dong, S.; Cui, X.; Zhong, S.; Gao, Y.; Wang, H. *Mol. Simulat.* **2011**, *37*, 1014.
35. Gu, C.; Gu, H.; Lang, M. *Macromol. Theory Simulat.* **2013**, *22*, 377.
36. Huang, Z.-M.; Zhang, Y. Z.; Kotaki, M.; Ramakrishna, S. *Compos. Sci. Technol.* **2003**, *63*, 2223.
37. Greiner, A.; Wendorff, J. H. *Chem. Int. Ed.* **2007**, *46*, 5670.
38. Koski, A.; Yim, K.; Shivkumar, S. *Mater. Lett.* **2004**, *58*, 493.
39. Thompson, C.; Chase, G.; Yarin, A.; Reneker, D. *Polymer* **2007**, *48*, 6913.
40. Fong, H.; Chun, I.; Reneker, D. H. *Polymer* **1999**, *40*, 4585.
41. Lim, C.; Tan, E.; Ng, S. *Appl. Phys. Lett.* **2008**, *92*, 141908.
42. Wang, C.; Hsu, C.-H.; Lin, J.-H. *Macromolecules* **2006**, *22*, 7662.

43. Patel, H. N.; Garcia, R.; Schindler, C.; Dean, D.; Pogwizd, S. M.; Singh, R.; Vohra, Y. K.; Thomas, V. *Polym. Int.* **2015**, *64*, 547.

44. Budkowski, A.; Hamley, I. W.; Koike, T. *Interfaces Crystallization Viscoelasticity*, Advances in Polymer Science; Springer-Verlag Berlin and Heidelberg GmbH & Co. KG.: Berlin, Germany, **2003**.

45. Zhang, F.; Stühn, B. *Colloid Polym. Sci.* **2007**, *285*, 371.

46. Reneker, D. H.; Chun, I. *Nanotechnology* **1996**, *7*, 216.

47. Reneker, D. H.; Yarin, A. L.; Fong, H.; Koombhongse, S. *J. Appl. Phys.* **2000**, *87*, 4531.

48. Martins-Franchetti, S. M.; Egerton, T.; White, J. *J. Polym. Environ.* **2010**, *18*, 79.

49. Yang, F.; Wolke, J. G. C.; Jansen, J. A. *Chem. Eng. J.* **2008**, *137*, 154.

50. Luong-Van, E.; Grondahl, L.; Chua, K. N.; Leong, K. W.; Nurcombe, V.; Cool, S. M. *Biomaterials* **2006**, *27*, 2042.

51. Shalumon, K.; Anulekha, K.; Chennazhi, K.; Tamura, H.; Nair, S.; Jayakumar, R. *Int. J. Biol. Macromol.* **2011**, *48*, 571.

52. Dumont, D.; Seveno, D.; De Coninck, J.; Bailly, C.; Devaux, J.; Daoust, D. *Polym. Int.* **2012**, *61*, 1263.